Blocking A1 astrocyte conversion with semaglutide attenuates blood-brain barrier disruption in mice after middle cerebral artery occlusion

Qi Zhang
Shanghai Jiao Tong University
Chang Liu
Shanghai Jiao Tong University
Rubing Shi
Shanghai Jiao Tong University
Huimin Shan
Shanghai Jiao Tong University
Lidong Deng
Shanghai Jiao Tong University
Tingting Chen
Shanghai Jiao Tong University
Zhijun Zhang
Shanghai Jiao Tong University
Guo-Yuan Yang
Shanghai Jiao Tong University
Yongting Wang
Shanghai Jiao Tong University
Yaohui Tang (yaohuitang@sjtu.edu.cn)
Shanghai Jiao Tong University https://orcid.org/0000-0002-9603-2650

Research Article

Keywords: A1 astrocyte, blood-brain barrier, ischemia, neuroinflammation, stroke

Posted Date: April 22nd, 2021

DOI: https://doi.org/10.21203/rs.3.rs-434590/v1

Abstract

Background

Astrocytes play an essential role in the modulation of blood-brain barrier function. Neurological diseases induce astrocytes to transform into a neurotoxic A1 phenotype, thus exacerbating brain injury. However, the effect of A1 astrocyte on the function of BBB after stroke is unknown.

Method:

Adult male ICR mice (n = 78) were subjected to 90-minute transient middle cerebral artery occlusion. Immunohistochemical staining of A1 (C3d) and A2 (S100A10) was performed to characterize phenotypic changes of astrocytes overtime after stroke. Glucagon-like peptide-1 receptor agonist semaglutide was intraperitoneally injected into the mice to inhibit A1 astrocyte. Infarct volume, atrophy volume, neurobehavioral outcomes, and BBB permeability were examined. RNA-seq was adopted to explore the potential targets and signaling pathways of A1 astrocytes induced BBB dysfunction.

Results

Astrocytes assumed the A2 phenotype at the early stage of ischemic stroke but gradually transformed to the A1 phenotype. Semaglutide treatment reduced M1 microglia polarization and A1 astrocytes conversion after ischemic stroke ($p < 0.05$). Ischemia induced brain infarct volume, atrophy volume and neuroinflammation were reduced in the semaglutide treated mice. Neurobehavioral outcomes were improved compared to the control mice ($p < 0.05$). Further study demonstrated that semaglutide treatment reduced the gap formation of tight junction proteins ZO-1, claudin-5 and occludin, as well as IgG leakage following three days of ischemic stroke ($p < 0.05$). *In vitro* experiments revealed that A1 astrocyte-conditioned medium disrupted BBB integrity. RNA-seq further showed that A1 astrocytes were enriched in inflammatory factors and chemokines, as well as significantly modulating TNF and chemokine signaling pathways, which are closely related to barrier damage.

Conclusion

We concluded that astrocytes undergo a conversion from A2 phenotype to A1 phenotype overtime after ischemic stroke. A1 astrocytes aggravated BBB disruption, suggesting that block of A1 astrocytes conversion provides a novel strategy for the treatment of ischemic stroke.

Introduction

Ischemic stroke is one of the leading causes of morbidity and mortality worldwide. Many pathological processes are involved in stroke progression, including blood-brain barrier (BBB) dysfunction,

inflammation [1], excitotoxicity, oxidative stress, neuronal loss, and glial activation. Glial cells, the largest cell population in the central nervous system (CNS) [2], have received extensive attention for their activation in response to CNS injury and subsequent conversion to different phenotypes, including neurotoxic and neuroprotective properties.

Astrocytes play critical roles in maintaining the essential function of the CNS. Astrocytes instruct the formation and elimination of synapses during development [3, 4], provide trophic factors to support neuronal function [5], mediate the uptake and recycling of neurotransmitters [6], form the structure of the brain, and are also involved in the maintenance of the BBB integrity [7]. It is clear that astrocytes dysfunction is closely related to the pathogenesis of many disease, including ischemic stroke. Accumulating evidence demonstrates that astrocytes could have different phenotypes. It has been reported that reactive astrocytes can be classified into A1 and A2 phenotypes, which have neurotoxic and neuroprotective effects, respectively [8, 9]. A1 astrocyte was induced by interleukin-1 alpha (IL-1α), tumor necrosis factor alpha (TNFα), and the classical complement component C1q, which were secreted by activated microglia. Evidence showed that A1 astrocytes lost many normal astrocyte functions such as promoting neuronal survival, inducing synapse formation and function and phagocytizing synapse, as well as releasing toxic factors to kill neurons and oligodendrocytes [10]. However, a comprehensive characterization of astrocyte phenotype conversion and the effects of A1 astrocytes on the BBB function after ischemic stroke are still unclear.

BBB is a highly complex and dynamic structure composed of tight junctions between endothelial cells lining blood vessels, astrocytic endfeet and a basement membrane, which plays a key role in regulating CNS homeostasis [11, 12]. It is well established that BBB is disrupted after ischemic stroke, which contributes to the development of brain injury and subsequent neurological impairment [13, 14]. Astrocytes directly encircled cerebral microvessels and modulated BBB functions via astrocyte-derived factors and endfeet [15, 16]. Reactive astrocytes secreted not only vascular permeability factors to down-regulate tight junction proteins, but also protective factors to protect endothelial cells from apoptosis, suggesting that astrocytes have dual effects on BBB after CNS injury [17]. Therefore, it is critical to elucidate the role of different phenotypes of astrocytes, especially A1 phenotype, on BBB integrity after ischemic stroke. Novel therapeutic strategies that attenuate BBB dysfunction by reversing A1 astrocytes are potential treatment options after ischemic stroke.

In this study, we aim to explore the effect of A1 astrocyte on the BBB integrity after ischemic stroke. We showed for the first time that ischemic stroke induced resting astrocyte (A0 astrocyte) converted into A2 astrocyte at the early stage, with a gradual shift to A1 astrocyte. *In vitro* studies revealed that A1 astrocyte conditioned medium disrupted BBB integrity, which was potentially mediated by inflammatory factors and chemokines secreted by A1 astrocyte. We also demonstrated that efficiently blocking A1 astrocytes conversion through semaglutide, a glucagon-like peptide-1 receptor (GLP-1R) agonist reduced ischemia induced BBB disruption, and improved neurobehavioral recovery. Our study highlighted a critical role of A1 astrocytes in the BBB integrity and concluded that A1 astrocyte was a potential therapeutic target for treating ischemic stroke.

Materials And Methods

Animal experiments

Experimental animal studies were performed according to the Animal Research: Reporting of *in vivo* Experiments (ARRIVE) guidelines. Animal experimental protocol was approved by the Institutional Animal Care and Use Committee (IACUC) of Shanghai Jiao Tong University, Shanghai, China. A total of 78 adult male ICR mice weighing 25-30 grams were purchased from Jie Si Jie Laboratory Animal Co., Ltd. (Shanghai, China) and housed in a standard facility with 12-hour light-dark cycle, free access to the food and water, ambient humidity of 20～50%, and temperature of 21～25°C. Mice were randomly assigned to 3 groups, sham group (n=12), transient middle cerebral artery occlusion (tMCAO) group (n=40) and tMCAO with semaglutide treated group (n=26). Experimental designs were summarized in **Fig. 1a**.

Transient middle cerebral artery occlusion (tMCAO)

The mouse model of tMCAO was established using a method described previously [18]. Briefly, mice were anesthetized with 1.5-2% isoflurane in a mixture of oxygen/nitrous oxide (30%/70%). First, the common carotid artery (CCA), internal carotid artery (ICA), and external carotid artery (ECA) were carefully separated. Then, a 6-0 nylon suture (Dermalon, 1756-31, Covidien) coated with silica gel was inserted through an incision in the ECA, into the ICA, and advanced until the suture tip reached the bifurcation of the middle cerebral artery (MCA). The inserted suture length was about 0.95 0.05 cm. The success of occlusion was confirmed by the decrease of surface cerebral blood flow (CBF) in the MCA territory to 20% of baseline CBF using a laser Doppler flowmetry (Moor Instruments, Devon, UK). Reperfusion was performed by withdrawing the suture 90 minutes after occlusion. The success of reperfusion was confirmed by more than 70% CBF recovered, compared to the baseline. Animals failed in occlusion or reperfusion were excluded from the study.

Drug administration

Semaglutide was purchased from China peptides Ltd. Company (Shanghai, China). The amino acid sequence of semaglutide is HXEGTFTSDVSSYLEGQAAKN6-(N-(17-carboxy-1-oxoheptadecyl)-L-gammaglutamyl-2-(2-(2-aminoethoxy)ethoxy)acetyl-2-(2-(2-aminoethoxy) ethoxy)acetyl)EFIAWLVRGRG-OH [19]. The semaglutide treated mice received 200 µl of semaglutide solution at a dose of 30 mg/kg at 2 hours after reperfusion via intraperitoneal (i.p.) injection, followed by the same dose injection every 5 days. The control group received 200 µl of PBS i.p. injection at 2 hours after reperfusion, followed by the same dose injection every 5 days.

Neurobehavioral assessment

Neurobehavioral tests were carried out by an investigator blinded to the experimental design using the modified neurological severity score (mNSS), hanging wire test, and rotarod test. mNSS was performed at 1, 3, 7, 14, 21 and 28 days after tMCAO. Hanging wire test and rotarod test were carried out at 3, 7, 14 21 and 28 days after tMCAO. mNSS was a composite score of motor, reflex, and balance tests. The severity

score was graded at a scale from 0 to 14, where 0 represents normal and 14 indicates the most severe injury [20].

Hanging wire test was used to assess muscle function and motor coordination [21]. In the hanging test, mice were hung on a horizontal wire. The wire was 1.6 mm in diameter, 50 cm in length, and elevated at 30 cm above the floor. Each mouse was given a score of 10 at the beginning of the test. The mice were then scored based on the number of times they reached the terminal (earn one point) and the number of falls (loss one point) in 180 seconds. If the mouse reached the terminal without falling in one trial, no score was given or taken. Therefore, the highest score an animal could receive is 10. The average score of three 180-second tests was used for analysis. A Kaplan-Meier-like curve was created using the scores, in which 10 indicates best muscle function and motor coordination, while a lower score indicated worse muscle function and motor coordination. Holding impulse (s*g), which was calculated by multiplying body mass (g) and hanging time (s), was used as an outcome measure of overall limb strength.

Rotarod test was used to evaluate motor coordination and balance [22]. Mice were trained for 3 consecutive days before tMCAO. On the first and second day of training, the mice were placed on the non-rotating rod to adapt for 1 minute, then the rod was accelerated to 20 revolutions per minute (rpm) and maintained for 5 minutes. On the third day of training, baseline test after two training sessions was carried out. The rotating rod was accelerated to 40 rpm while the mice were monitored and the fell off rate within 5 minutes was recorded and analyzed.

Brain infarct volume and atrophy volume measurement

Six mice from each group were euthanized with an excess of 10% chloral hydrate at 3 days and 14 days after tMCAO. Mouse brain samples were collected after intracardial perfusion with 0.1 ml/L PBS followed by 4% paraformaldehyde (PFA, Sinopharm Chemical Reagent, Shanghai, China). Brains were immediately placed in 4% PFA for 6 hours at 4°C and then transferred to 30% sucrose in PBS until the brain sank to the bottom. Processed mouse brains were placed in −42°C pre-chilled isopentane for 10 min and then stored at −80°C. The pre-OCT-embedded brains were cut into floating coronal sections at a thickness of 30 μm from the anterior commissure to the hippocampus and stored in a 24-well plate containing antifreeze (Meilunbio, Dalian, China). Cresyl violet staining was carried out by sampling 16 sections spaced 300 μm apart that collectively spans the entire injury region for each mouse. The selected brain slices were mounted on glass slides and air dried. The sections were then stained in 0.1% Cresyl violet solution (Meilunbio, Dalian, China) followed by de-staining in ethyl alcohol. The ratio of staining in the ipsilateral and contralateral hemispheres was calculated using ImageJ (National Institutes of Health, Bethesda, MD).

Infarct volume were calculated by the following formula: $V = \sum h/3 * [\Delta S_n + (\Delta S_n * \Delta S_{n+1})^{1/2} + \Delta S_{n+1}$, V represents volume. ΔS were calculated by subtracting the normal area of the ipsilateral hemisphere from the contralateral hemisphere area. ΔSn and $\Delta Sn+1$ represent the infarct areas of two adjacent sections. h represents the thickness between two adjacent brain slices sampled (h=300 μm) [23].

Immunostaining and quantification

Brain slices or cell slides were fixed with 4% PFA for 10 minutes and incubated in 0.3% Triton X-100 solution for 10 minutes followed by blocking with 10% BSA for 1 hour at room temperature. Astrocytes were incubated with antibodies against C3d (1:100, AF2655, R&D system, Minneapolis, MN), S100A10 (1:100, AF2377, R&D system), and glial fibrillary acidic protein (GFAP, 1:200, AB5804, Millipore, Burlington, MA). Microglia were incubated with antibodies against Iba-1 (1:200, NB100-1028, Novusbio, CO), CD16/32 (1:200, 553141, Thermo fisher scientific, MA), and Arginase (1:200, SC-271430, Santa Cruz Biotechnology, CA). Brain sections were incubated with antibodies against occludin (1:100, 33-1500, Invitrogen, Carlsbad, CA), ZO-1 (1:100, 61-7300, Invitrogen), claudin-5 (1:100, 35-2500, Invitrogen), CD31 (1:200, AF806, R&D Systems) overnight at 4°C. After being washed three times in PBS, brain sections and cell slides were incubated with fluorescent conjugated secondary antibodies for 1 hour at 37°C. The fluorescent images were collected with a TCS SP5 Confocal Scanning System (Leica, Solms, Germany).

Brain sections stained for occludin, ZO-1, or claudin-5 were analyzed for tight junction gap length, which was presented as a percentage (%) of whole tight junction staining. GFAP staining results were analyzed by comparing the GFAP integral optical density (IOD). The number of C3d-positive, S100A10-positive, CD16/32-positive, GFAP-labelled, and IBA-1 labeled cells was counted from randomly selected fields in the peri-focal striatum of the ipsilateral hemisphere in three mice from each group. For each mouse, four-section were evaluated and three fields per section were sampled. The data were analyzed using ImageJ (National Institutes of Health, MD) and Prism Graphpad 8 (GraphPad Software, San Diego).

Western blotting analysis

The ischemic tissue from the ipsilateral hemisphere of the striatum was dissected and lysed in the protein lysis buffer (RIPA, protease cocktail inhibitor and phosphatase inhibitor) on ice immediately after brain sample collection [24]. The protein concentration of each protein sample was determined by a BCA kit (Meilunbio, Dalian, China). An aliquot of 30 μg of total protein from each sample was loaded onto 12% sodium dodecyl sulfate-polyacrylamide gel electrophoresis (SDS-PAGE) gel and subjected to electrophoresis. The protein samples on the SDS-PAGE gel were transferred to polyvinylidene fluoride membrane (Merck KGaA, Darmstadt, Germany). The membrane was blocked with 5% non-fat milk for 1 hour at room temperature and incubated with the primary antibodies against GFAP (1:4000, AB5804, Millipore, MA), C3d (1:1000, AF2655, R&D system), and β-actin (1:1000, 66009, Invitrogen) overnight at 4°C. After being washed three times in TBST buffer (Meilunbio), the membranes were incubated with HRP-conjugated secondary antibody for 1 hour at room temperature. Immunoblots were developed by incubating with solutions from an enhanced chemiluminescence kit (ECL, Pierce). The results of ECL were analyzed using Image J software.

Real-Time PCR Analysis

The ischemic tissue extracted from the ipsilateral hemisphere of the striatum was used to isolate total RNA using TRIzol reagent (Invitrogen). The Extracted RNA was used for real-time PCR analysis to detect

the expression levels of IL-1α, TNFα, and C1q. Single-strand cDNA was synthesized through a universal cDNA synthesis kit (Qiagen, Hilden, Germany) under the conditions of 42°C for 1 hour and then 95°C for 5 minutes. The expression of RNA was tested by a fast real-time PCR system (7900 HT, ABI, Foster City, CA) using an SYBR Green master mix (Qiagen) with the following cycling conditions: 95°C for 10 minutes followed by 40 cycles of 95°C for 10 seconds and 60°C for 1 minute. GAPDH was used as the control for tissues. The primers used for real-time PCR analysis are listed in **Table 1**.

Primary microglia and astrocyte cell cultures

Primary microglia and astrocytes were isolated from postnatal ICR mice (JieSiJie, Shanghai, China). Briefly, the cortex was isolated from the brain of mice and then trypsinized for 10 minutes. After centrifugation, the cell pellet was resuspended in glial cell culture medium with 10% inactivated fetal bovine serum, filtered with a 70 μm filter (Millipore), and then inoculated on the culture dish prepared in advance. The mixed glial cells were kept in an incubator at 37°C and cultured for 10 days under the conditions of 95% humidity and 5% CO_2. When the astrocytes were confluent, the primary microglia were isolated from the culture by briefly shaking. To obtain primary astrocytes, mixed glial cells were seeded into the petri dish and the medium was replaced with fresh culture medium every 3 days. A1 astrocytes were obtained by treating primary astrocytes with IL-1α (3 ng/ml, I3901, Sigma, MO), TNF (30 ng/ml, 8902SF, Cell Signaling Technology, MA), and C1q (400 ng ml−1, MBS143105, MyBio Source, CA) for 24 hours *in vitro.*

Culture of bEnd.3 cells with different types of astrocyte conditioned medium

Mouse brain capillary endothelial cell line (bEnd.3) cells were cultured under normal culture conditions, and then were cultured with different types of astrocyte-conditional medium (ACM) for 24 hours to prepare for the subsequent experiments. The sources of ACM included medium from the resting A0 astrocytes (A0-CM), from the A1 astrocytes (A1-CM) and from astrocytes treated with medium derived from LPS stimulated microglia (LPS-MCM-AS-CM).

RNA sequencing and differentially expressed gene analysis

Total RNA was extracted from cells using Trizol (Invitrogen). RNA purity and quantification were evaluated using the NanoDrop 2000 spectrophotometer (Thermo Scientific, USA). The libraries were constructed using TruSeq Stranded mRNA LT Sample Prep Kit (Illumina, San Diego, CA). The transcriptome sequencing and analysis were conducted by OE Biotech Co., Ltd. (Shanghai, China). The genome-wide transcriptomic analysis was performed on 4 independent experiments in the A0 astrocytes and A1 astrocytes groups. Differential expression analysis was performed using the DESeq (2012) R package. $p<0.05$ and fold change>2 or fold change<0.5 were set as the threshold for significantly differential expression. Gene set enrichment analysis (GSEA; https://www.broadinstitute.org/gsea/index.jsp) was performed to find differential phenotypes between A0 astrocytes and A1 astrocytes groups.

Statistical analysis

The parametric data were analyzed using Prism Graphpad 8. Comparisons between two groups were carried out using Student's *t*-test. For comparison among multiple groups, statistical significance between each group were examined by one-way ANOVA followed by Bonferroni correction for multiple analyses. All data were expressed as mean±standard error of the mean (SEM), and two-tail $p<0.05$ was considered statistically significant [25].

Results

Ischemic stroke induced A1 astrocytes formation

To determine if ischemia initiates astrocytes conversion, we characterized the phenotypic changes of astrocytes at different time points after tMCAO. We found that the number of $C3d^+/GFAP^+$ cells at the ischemic perifocal region was gradually increased from day 1 to day 14, while the number of $S100A10^+/GFAP^+$ cells was gradually decreased (**Fig. 1b**). The percentage of $C3d^+/GFAP^+$ cells reached 60% of total cells, in comparison, $S100A10^+/GFAP^+$ cells decreased to 40% of total cells at 14 days of tMCAO, indicating that ischemia could promote resting astrocytes transform to the A1 or A2 phenotype astrocytes dynamically. Besides, we found that at the third day after tMCAO, the A1 astrocytes endfeet wrapped surrounding the microvessels in the peri-focal region (**Fig. 1c**), suggesting a crosstalk between A1 astrocytes and endothelial cells during tMCAO.

Semaglutide reduced M1 microglia polarization and A1 astrocytes formation after ischemic stroke

GLP1R agonists have been proven as potential anti-inflammatory agents [26]. Thus, we hypothesized that GLP1R agonists could block A1 astrocytes formation and microglia polarization towards the M1 phenotype microglia. To test our hypothesis, we injected semaglutide, a GLP1R agonist, into ischemic mice 2 hours after tMCAO. We found that semaglutide treatment significantly reduced the number of $Iba\text{-}1^+$ cells compared to the control at day 3 after tMCAO ($p<0.01$, **Fig. 2a**). Besides, semaglutide treatment reduced the number of $CD16/32^+/Iba\text{-}1^+$ cells compared to the control ($p<0.05$, **Fig. 2a**), suggesting that semaglutide attenuated microglia M1 polarization in the acute phase after ischemic brain injury.

It has been reported that IL-1α, TNFα and C1q together trigger A1 conversion of reactive astrocytes, and subsequently cause neuronal death. Therefore, we examined the expression of IL-1α, TNFα and C1q after tMCAO. Real time-PCR analysis of the perifocal region of the ipsilateral hemisphere revealed that tMCAO induced IL-1α, TNFα and C1q hyperexpression (**Fig. 2b)**, and the IL-1α, TNFα and C1q expression were reduced in the semaglutide treated mice compared to the control ($p<0.05$, **Fig. 2b**). To validate if semaglutide could reduce A1 astrocytes formation, western blot and immunofluorescence staining were performed to detect C3d, S100A10 and GFAP protein levels. We found that the A1 astrocytic marker C3d and GFAP expression increased apparently after ischemic brain injury ($p<0.001$, **Fig. 3a, b**), and semaglutide treatment decreased their expression at day 3 after tMCAO ($p<0.01$, **Fig. 3a, b**), suggesting

semaglutide could reduce A1 astrocytes after tMCAO. In contrast, the expression of A2 astrocytes marker S100A10 increased significantly in the semaglutide treatment group at day 3 after injury (p<0.05, **Fig. 3a, b**).

Inhibiting A1 astrocyte transformation reduced brain infarct volume and improved neurobehavioral outcomes after tMCAO in mice

To demonstrate the effect of blocking A1 astrocytes on infarction and neurobehavioral recovery of stroke mice, we examined infarct volume and neurobehavioral tests including mNSS score, rotarod test and hanging wire test in tMCAO mice. We found that infarct volume was greatly decreased in the semaglutide treated mice compared to the control at day 3 of tMCAO (p<0.05, **Fig. 4a**). Similarly, atrophy volume was reduced in the semaglutide treated mice compared to the control at 28 days of tMCAO (p<0.01, **Fig. 4b**). We found that the mNSS score was lower in the semaglutide treated mice compared to the control at 1, 3, 7, 14, 21 and 28 days following tMCAO (p<0.05, **Fig. 4c**). Furthermore, the performance of motor functions in rotarod test and hanging wire test were better in the semaglutide treated mice compared to the control mice (p<0.05, **Fig. 4d, f**). The changes of body weight in the semaglutide treated mice were significantly recovered at 21 and 28 days of tMCAO (p<0.05, **Fig. 4g**), suggesting that the general condition was also improved in semaglutide treated mice after tMCAO.

Inhibiting A1 astrocyte transformation attenuated BBB disruption after tMCAO in mice

To evaluate the effect of A1 astrocytes on the BBB after tMCAO, we examined the IgG leakage in the mouse brain at 3 days after tMCAO. The results showed that IgG leakage reduced in the ipsilateral hemisphere in semaglutide treated mice compared to the controls (p<0.01, **Fig. 5a**). Immunostaining of tight junction proteins, including occludin, ZO-1 and claudin-5, in combination with endothelial cell marker CD31 was used to assess endothelial tight junction gap formation. We found that the disruption of such arrangement and microvessel gap formation was observed in the perifocal region of tMCAO mouse brain. However, the distance of gap formation revealed was less in the semaglutide treated mice compared to the control (p<0.05, **Fig. 5b**), suggesting a reduction of tight junction gap formation in the perifocal region in the acute phase after tMCAO.

A1 astrocytes derived medium reduced tight junction protein expression of endothelial cells *in vitro*

It was previously reported that IL-1α, TNFα and C1q are required for converting resting A0 astrocytes to A1 astrocytes [9]. As our immunofluorescence staining images and real-time PCR results showed that IL-1α, TNFα and C1q treatment increased the expression of A1 astrocytes marker C3d in astrocytes, as well as A1 astrocytes related genes including H2-T23, Serping1, H2D1 and Ligp1 (p<0.01, **Fig. 6a, b**), suggesting that we successfully induced A1 astrocytes *in vitro*.

To investigate the effect of A1 astrocytes on tight junction proteins of endothelial cells, bEnd.3 cells were treated with medium from A0 astrocytes (A0-CM), or medium from A1 astrocytes (A1-CM) or medium from astrocytes that were treated with LPS stimulated microglia (LPS-MCM-AS-CM). We found that A1-

CM treatment and LPS-MCM-AS-CM treatment reduced the ZO-1 and claudin-5 expression in endothelial cells compared to the control (A0-CM treatment) (**Fig. 6c, d**).

A1 astrocytes upregulated inflammation-, immune- and chemotaxis-related signaling pathways

To explore the underlying molecular mechanisms of how A1 astrocytes disrupt BBB integrity, we analyzed transcriptome differences between A1 astrocytes and A0 astrocytes. We found that 2474 genes showed differentially expressed genes (fold change>2) in A1 astrocytes, among which1085 genes were up-regulated and 1389 genes were down-regulated (**Fig. 7a**). Among them, BBB breakdown related genes including Matrix metalloproteinase-3 (MMP-3) and MMP-9 were highly upregulated (**Suppl. table 1**).

Gene Ontology (GO) pathway enrichment analyses of the upregulated genes showed that compared to A0 astrocytes, multiple altered biological processes including T cell differentiation, immune response, inflammatory response and chemokine-mediated signaling pathway were increased in A1 astrocytes **(Fig. 7b**). KEGG analyses further demonstrated altered canonical signaling pathways that related to inflammation, chemokine signaling and immune response in A1 astrocytes were enriched (**Fig. 7c**). Many inflammatory factors and chemokines were found upregulated in A1 astrocytes (**Suppl. table 1**), indicating A1 astrocytes may induce inflammatory and immune responses to disrupt BBB integrity after stroke.

Discussion

In present study, we demonstrated that the number of A1 astrocytes increased within 14 days after tMCAO while A2 astrocytes decreased during this time. Semaglutide treatment reduced M1 microglia polarization and A1 astrocytes transformation, and subsequently reduced brain infarct volume, improved neurobehavioral outcomes, reduced neuroinflammation, and attenuated BBB disruption in tMCAO mice. Further RNA-seq study found inflammation-, immune- and chemotaxis-related signaling pathways involved in A1 astrocytes function. Our results suggested that A1 astrocyte was a specific cell group, which played an important role in BBB integrity. Inhibiting A1 astrocyte conversion provides a novel approach for ischemic stroke therapy.

It is well known that astrocytes play essential roles in the formation and maintenance of the BBB [27–29]. Accumulating evidence demonstrated that the heterogeneity of astrocytes existed in CNS, both morphologically and functionally [30–32]. In particular, the recently proposed disease-associated astrocytes attracted widespread attention [33]. IL-1α, TNFα, and C1q could activate astrocytes to transform into a neurotoxic A1 phenotype [9]. However, its effect on BBB integrity was largely unexplored. Using a tMCAO model, we demonstrated that resting A0 astrocyte transformed into A1 phenotype after tMCAO, and the number of A1 astrocytes increased over time, while inhibition of A1 astrocytes transformation by semaglutide attenuated BBB disruption. The results of *in vitro* experiments showed that conditional medium from A1 astrocytes reduced tight junction protein expression in endothelial cells, suggesting the destructive effect of A1 astrocytes on the BBB integrity.

IL-1α, TNFα and C1q are three inflammatory factors that are specifically expressed in microglia, and they are required for the A1 astrocyte transformation [10]. Our study showed that IL-1α, TNFα, and C1q were highly upregulated in the brain at 3 days after tMCAO, and an increase of A1 astrocytes transformation was detected in the perifocal area after ischemic stroke, while such phenomenon was absent in the normal brain, indicating that ischemic stroke activated microglia could release these cytokines, and promote resting A0 astrocyte towards A1 astrocytes transformation. Our *in vitro* study further showed that adding IL-1α, TNFα and C1q into the medium of resting astrocytes could promote them to A1 astrocyte transformation.

Astrocytes play important roles in maintaining BBB integrity by safeguarding endothelial tight junctions [34–36]. We found that 3 days after ischemic stroke, a large number of A1 astrocytes endfeet wrapped surround the wall of blood vessels, leading us to suspect the potential crosstalk between A1 astrocytes and endothelial cells, which may affect BBB integrity. Our data strongly supported the hypothesis as conditional medium derived from A1 astrocytes or LPS-MCM treated astrocytes reduced tight junction proteins in endothelial cells, suggesting toxic factors secreted from A1 astrocytes degrade tight junction proteins.

To gain insight into what are the A1 astrocytes derived toxic factors that disrupt BBB integrity, transcriptomic analyses of A0 and A1 astrocytes were performed. Our data suggested that multiple biological processes related to BBB function were increased in A1 astrocytes. Growing evidence has shown that inflammatory and immune response are two key driving forces that critically affect BBB function after stroke. Inflammation is involved in tight junction decomposition which ultimately causes BBB breakdown. We demonstrated that TNF, IL-17 and NF-kappa B signaling pathways were enriched in A1 astrocytes, and many inflammatory factors such as TNF and IL-6 were increased. It should be noted that matrix metalloproteinases (MMPs) including MMP9, MMP14 and MMP3 were highly upregulated in A1 astrocytes. MMPs are zinc-dependent endopeptidases produced by astrocytes, microglia, endothelial cells that degrade extracellular matrix proteins during ischemic stroke [37]. MMP9 and MMP3 are reported to have detrimental effects on BBB integrity. Blocking MMP9 and MMP3 significantly attenuate BBB disruption and improve neurobehavioral recovery [38]. A1 astrocytes may induce BBB disruption by MMP9 and MMP3, as we found MMP9 and MMP3 were upregulated in A1 astrocytes.

In addition to inflammatory response, chemokine signaling pathways and chemokines including CCL12, CCL5, CXCL1, CXCL2 and CXCL10 were also enriched in A1 astrocytes. These chemokines are well known for mediating inflammatory and immune responses by guiding immune cells migration into the lesion area of the brain. For example, CCL5 is a chemoattractant of T cells to the site of inflammation, which mediates the cerebral inflammation and causes BBB disruption [39]. CXCL1 produced by astrocytes is a critical ligand required for neutrophil trans-endothelial migration and exacerbates brain damage[40]. Activating MMPs degraded endothelial cell tight junction proteins, secreted inflammatory cytokines and adhesion molecules, and induced endothelial cell death [37]. All these processes are closely related to the BBB disruption.

Besides A1 astrocyte, A2 astrocyte was also detected in the brain after ischemic stroke. Previous studies showed that activated astrocytes promoted neuronal function recovery and repair [41–43]. A2 astrocyte could up-regulate neurotrophic factors and vascular growth factors, which presumably promoted neuronal survival, aided axon regeneration, and promoted BBB repair [44]. Therefore, manipulation of astrocyte phenotype was regarded as a potential therapeutic strategy. Understanding the heterogeneity of astrocytes helps to comprehend how the function of astrocytes shapes the function and dysfunction of the brain.

GLP-1 is a 30-amino acid peptide hormone for stimulating insulin secretion. Currently, GLP-1 and GLP-1 receptor agonists including exendin-4, liraglutide, semaglutide, etc., were developed and approved for treating type 2 diabetes [45, 46]. In addition, recent studies demonstrated their potential for neurological disorders treatment [47]. In a recent study, semaglutide was shown to have neuroprotective effects in a rat MCAO model [19]. Besides, a study demonstrated that NLY01, a GLP1R agonist, protected against the death of dopaminergic neurons and improved behavioral recovery in Parkinson's disease, which was mediated by the block of A1 astrocyte transformation [9]. In the present study, we found that similar to NLY01, semaglutide could also reduce A1 astrocyte transformation. This may be caused by attenuation of microglial inflammation as semaglutide treatment reduced expression of IL-1α, TNFα, and C1q and M1 microglial polarization. Together, these results highlighted the important role of A1 astrocytes on the BBB disruption after ischemic stroke.

Conclusions

Our study demonstrated that stroke induced A1 astrocyte disrupted blood-brain barrier integrity, and block of A1 astrocytes conversion by semaglutide attenuated brain injury, suggesting the detrimental role of A1 astrocyte in stroke. We can envision that A1 astrocytes to be a novel therapeutic target for the ischemic stroke therapy.

Abbreviations

ACM
astrocyte-conditioned medium;
A0-CM
A0 astrocyte-conditioned medium;
A1-CM
A1 astrocyte-conditioned medium;
BBB
blood-brain barrier;
BCA
bicinchoninic acid;
bEnd.3
brain-derived Endothelial cells.3;

BSA
bull serum albumin;
CBF
cerebral blood flow;
CD31
cluster of differentiation 31;
CNS
central nervous system;
C1q
complement component 1, subcomponent q;
DAPI
4',6-Diamidino-2-phenylindoledihydrochloride;
GSEA
Gene Set Enrichment Analysis;
GFAP
glial fibrillary acidic protein;
GLP1R
glucagon-like peptide-1 receptor;
GO
Gene Ontology;
Iba-1
Ionized calcium bindingadaptor molecule-1;
IL-1α
interleukin-1 alpha;
IOD
integral optical density;
KEGG
Kyoto Encyclopedia of Genes and Genomes;
LPS
lipopolysaccharides;
SEM
mean ± standard error of the mean;
MMPs
matrix metalloproteinases;
mNSS
modified neurological severity score;
mRNA
messenger ribonucleic acid;
tMCAO
transient middle cerebral artery occlusion;

TNFα
tumor necrosis factor alpha.

Declarations

Ethics approval

Animal protocol was approved by the Institutional Animal Care and Use Committee (IACUC) of Shanghai Jiao Tong University, Shanghai, China. All animal procedures were performed to minimize pain or discomfort in accordance with current protocols.

Consent for publication

Not applicable.

Availability of data and materials:

The datasets used and/or analyzed during the current study are available from the corresponding author on reasonable request.

Competing interests:

No competing interest.

Funding

This study was supported by grants from the National Natural Science Foundation of China (NSFC) projects 81801170 (YT), 82071284 (YT), 81870921 (YW), 81771251 (GYY), 81771244 (ZZ), 81974179 (ZZ), National Key R&D Program of China #2016YFC1300602 (GYY), #2019YFA0112000 (YT), the Scientific Research and Innovation Program of Shanghai Education Commission 2019-01-07-00-02-E00064 (GYY), Science and Technological Innovation Act Program of Shanghai Science and Technology Commission, 20JC1411900 (GYY), the Science and Technology Opening Program of the Education Ministry of Henan Province (182106000061, GYY) and K. C. Wong Education Foundation (GYY).

Author’s contributions

QZ and CL participated in the research design, all experimental procedures, animal surgery, RNA seq, data analysis and drafting of the first manuscript. RS, HS and LD contributed to animal surgery, behavioral tests and data collection. TC assisted with data collection. ZZ and GYY were involved in the discussion of the research design, the results and edited the manuscript. YW and YT supervised all aspects including research design, data analysis and manuscript preparation.

Acknowledgements

The authors would like to thank Dr. Qidong Zu (OE Biotech, Inc., Shanghai, China, http://www.oebiotech.com/) for assistance with the bioinformatics analysis of RNA-seq.

References

1. Li X, Liao Y, Dong Y, Li S, Wang F, Wu R, et al. Mib2 Deficiency Inhibits Microglial Activation and Alleviates Ischemia-Induced Brain Injury. Aging Dis. 2020;11(3):523–35.
2. Shetty AK, Upadhya R, Madhu LN, Kodali M. Novel Insights on Systemic and Brain Aging, Stroke, Amyotrophic Lateral Sclerosis, and Alzheimer's Disease. Aging Dis. 2019;10(2):470–82.
3. Allen NJ, Bennett ML, Foo LC, Wang GX, Chakraborty C, Smith SJ, et al. Astrocyte glypicans 4 and 6 promote formation of excitatory synapses via GluA1 AMPA receptors. Nature. 2012;486(7403):410–4.
4. Chung WS, Clarke LE, Wang GX, Stafford BK, Sher A, Chakraborty C, et al. Astrocytes mediate synapse elimination through MEGF10 and MERTK pathways. Nature. 2013;504(7480):394–400.
5. Banker GA. Trophic interactions between astroglial cells and hippocampal neurons in culture. Science. 1980;209(4458):809–10.
6. Rothstein JD, Dykes-Hoberg M, Pardo CA, Bristol LA, Jin L, Kuncl RW, et al. Knockout of glutamate transporters reveals a major role for astroglial transport in excitotoxicity and clearance of glutamate. Neuron. 1996;16(3):675–86.
7. Bush TG, Puvanachandra N, Horner CH, Polito A, Ostenfeld T, Svendsen CN, et al. Leukocyte infiltration, neuronal degeneration, and neurite outgrowth after ablation of scar-forming, reactive astrocytes in adult transgenic mice. Neuron. 1999;23(2):297–308.
8. Liddelow SA, Guttenplan KA, Clarke LE, Bennett FC, Bohlen CJ, Schirmer L, et al. Neurotoxic reactive astrocytes are induced by activated microglia. Nature. 2017;541(7638):481–7.
9. Yun SP, Kam TI, Panicker N, Kim S, Oh Y, Park JS, et al. Block of A1 astrocyte conversion by microglia is neuroprotective in models of Parkinson's disease. Nat Med. 2018;24(7):931–8.
10. Guttenplan KA, Weigel MK, Adler DI, Couthouis J, Liddelow SA, Gitler AD, et al. Knockout of reactive astrocyte activating factors slows disease progression in an ALS mouse model. Nat Commun. 2020;11(1):3753.
11. Sweeney MD, Zhao Z, Montagne A, Nelson AR, Zlokovic BV. Blood-Brain Barrier: From Physiology to Disease and Back. Physiol Rev. 2019;99(1):21–78.
12. Serlin Y, Shelef I, Knyazer B, Friedman A. Anatomy and physiology of the blood-brain barrier. Semin Cell Dev Biol. 2015;38:2–6.
13. Jiang X, Andjelkovic AV, Zhu L, Yang T, Bennett MVL, Chen J, et al. Blood-brain barrier dysfunction and recovery after ischemic stroke. Prog Neurobiol. 2018;163–164:144 – 71.
14. Prakash R, Carmichael ST. Blood-brain barrier breakdown and neovascularization processes after stroke and traumatic brain injury. Curr Opin Neurol. 2015;28(6):556–64.

15. Abbott NJ, Patabendige AA, Dolman DE, Yusof SR, Begley DJ. Structure and function of the blood-brain barrier. Neurobiol Dis. 2010;37(1):13–25.
16. Guérit S, Fidan E, Macas J, Czupalla CJ, Figueiredo R, Vijikumar A, et al. Astrocyte-derived Wnt growth factors are required for endothelial blood-brain barrier maintenance. Prog Neurobiol. 2021;199:101937.
17. Alvarez JI, Katayama T, Prat A. Glial influence on the blood brain barrier. Glia. 2013;61(12):1939–58.
18. Qu M, Pan J, Wang L, Zhou P, Song Y, Wang S, et al. MicroRNA-126 Regulates Angiogenesis and Neurogenesis in a Mouse Model of Focal Cerebral Ischemia. Mol Ther Nucleic Acids. 2019;16:15–25.
19. Yang X, Feng P, Zhang X, Li D, Wang R, Ji C, et al. The diabetes drug semaglutide reduces infarct size, inflammation, and apoptosis, and normalizes neurogenesis in a rat model of stroke. Neuropharmacology. 2019;158:107748.
20. Li Y, Chopp M, Chen J, Wang L, Gautam SC, Xu YX, et al. Intrastriatal transplantation of bone marrow nonhematopoietic cells improves functional recovery after stroke in adult mice. J Cereb Blood Flow Metab. 2000;20(9):1311–9.
21. Raymackers JM, Debaix H, Colson-Van Schoor M, De Backer F, Tajeddine N, Schwaller B, et al. Consequence of parvalbumin deficiency in the mdx mouse: histological, biochemical and mechanical phenotype of a new double mutant. Neuromuscul Disord. 2003;13(5):376–87.
22. Hamm RJ, Pike BR, O'Dell DM, Lyeth BG, Jenkins LW. The rotarod test: an evaluation of its effectiveness in assessing motor deficits following traumatic brain injury. J Neurotrauma. 1994;11(2):187–96.
23. Wen RX, Shen H, Huang SX, Wang LP, Li ZW, Peng P, et al. P2Y6 receptor inhibition aggravates ischemic brain injury by reducing microglial phagocytosis. CNS Neurosci Ther. 2020;26(4):416–29.
24. Shan HM, Zang M, Zhang Q, Shi RB, Shi XJ, Mamtilahun M, et al. Farnesoid X receptor knockout protects brain against ischemic injury through reducing neuronal apoptosis in mice. J Neuroinflammation. 2020;17(1):164.
25. Pan B, Lewno MT, Wu P, Wang X. Highly Dynamic Changes in the Activity and Regulation of Macroautophagy in Hearts Subjected to Increased Proteotoxic Stress. Front Physiol. 2019;10:758.
26. Lee YS, Jun HS. Anti-Inflammatory Effects of GLP-1-Based Therapies beyond Glucose Control. Mediators Inflamm. 2016;2016:3094642.
27. Abbott NJ. Astrocyte-endothelial interactions and blood-brain barrier permeability. J Anat. 2002;200(6):629–38.
28. Heithoff BP, George KK, Phares AN, Zuidhoek IA, Munoz-Ballester C, Robel S. Astrocytes are necessary for blood-brain barrier maintenance in the adult mouse brain. Glia. 2021;69(2):436–72.
29. Langen UH, Ayloo S, Gu C. Development and Cell Biology of the Blood-Brain Barrier. Annu Rev Cell Dev Biol. 2019;35:591–613.
30. Anderson MA, Ao Y, Sofroniew MV. Heterogeneity of reactive astrocytes. Neurosci Lett. 2014;565:23–9.

31. Ben Haim L, Rowitch DH. Functional diversity of astrocytes in neural circuit regulation. Nat Rev Neurosci. 2017;18(1):31–41.
32. Oberheim NA, Goldman SA, Nedergaard M. Heterogeneity of astrocytic form and function. Methods Mol Biol. 2012;814:23–45.
33. Liddelow SA, Barres BA. Reactive Astrocytes: Production, Function, and Therapeutic Potential. Immunity. 2017;46(6):957–67.
34. Ronaldson PT, Davis TP. Blood-brain barrier integrity and glial support: mechanisms that can be targeted for novel therapeutic approaches in stroke. Curr Pharm Des. 2012;18(25):3624–44.
35. Michinaga S, Koyama Y. Dual Roles of Astrocyte-Derived Factors in Regulation of Blood-Brain Barrier Function after Brain Damage. Int J Mol Sci. 2019;20(3).
36. Shindo A, Maki T, Mandeville ET, Liang AC, Egawa N, Itoh K, et al. Astrocyte-Derived Pentraxin 3 Supports Blood-Brain Barrier Integrity Under Acute Phase of Stroke. Stroke. 2016;47(4):1094–100.
37. Rempe RG, Hartz AMS, Bauer B. Matrix metalloproteinases in the brain and blood-brain barrier: Versatile breakers and makers. J Cereb Blood Flow Metab. 2016;36(9):1481–507.
38. Turner RJ, Sharp FR. Implications of MMP9 for Blood Brain Barrier Disruption and Hemorrhagic Transformation Following Ischemic Stroke. Front Cell Neurosci. 2016;10:56.
39. Sokol CL, Luster AD. The chemokine system in innate immunity. Cold Spring Harb Perspect Biol. 2015;7(5).
40. Michael BD, Bricio-Moreno L, Sorensen EW, Miyabe Y, Lian J, Solomon T, et al. Astrocyte- and Neuron-Derived CXCL1 Drives Neutrophil Transmigration and Blood-Brain Barrier Permeability in Viral Encephalitis. Cell Rep. 2020;32(11):108150.
41. Anderson MA, Burda JE, Ren Y, Ao Y, O'Shea TM, Kawaguchi R, et al. Astrocyte scar formation aids central nervous system axon regeneration. Nature. 2016;532(7598):195–200.
42. Sofroniew MV. Reactive astrocytes in neural repair and protection. Neuroscientist. 2005;11(5):400–7.
43. Pekny M, Pekna M. Astrocyte reactivity and reactive astrogliosis: costs and benefits. Physiol Rev. 2014;94(4):1077–98.
44. Liu Z, Chopp M. Astrocytes, therapeutic targets for neuroprotection and neurorestoration in ischemic stroke. Prog Neurobiol. 2016;144:103–20.
45. Nauck MA, Quast DR, Wefers J, Meier JJ. GLP-1 receptor agonists in the treatment of type 2 diabetes - state-of-the-art. Mol Metab. 2020:101102.
46. Shan Y, Tan S, Lin Y, Liao S, Zhang B, Chen X, et al. The glucagon-like peptide-1 receptor agonist reduces inflammation and blood-brain barrier breakdown in an astrocyte-dependent manner in experimental stroke. J Neuroinflammation. 2019;16(1):242.
47. Harkavyi A, Whitton PS. Glucagon-like peptide 1 receptor stimulation as a means of neuroprotection. Br J Pharmacol. 2010;159(3):495–501.

Table

Table 1. Primer sequences are listed as follows:

Gene	Forward primer	Reverse primer
IL1α	GCACCTTACACCTACCAGAGT	AAACTTCTGCCTGACGAGCTT
TNFα	ACCCTCACACTCAGATCATCTT	GGTTGTCTTTGAGATCCATGC
C1q	TCTGCACTGTACCCGGCTA	CCCTGGTAAATGTGACCCTTTT
H2-T23	GGACCGCGAATGACATAGC	GCACCTCAGGGTGACTTCAT
Serping1	ACAGCCCCCTCTGAATTCTT	GGATGCTCTCCAAGTTGCTC
H2-D1	TCCGAGATTGTAAAGCGTGAAGA	ACAGGGCAGTGCAGGGATAG
Ligp1	GGGGCAATAGCTCATTGGTA	ACCTCGAAGACATCCCCTTT

Figures

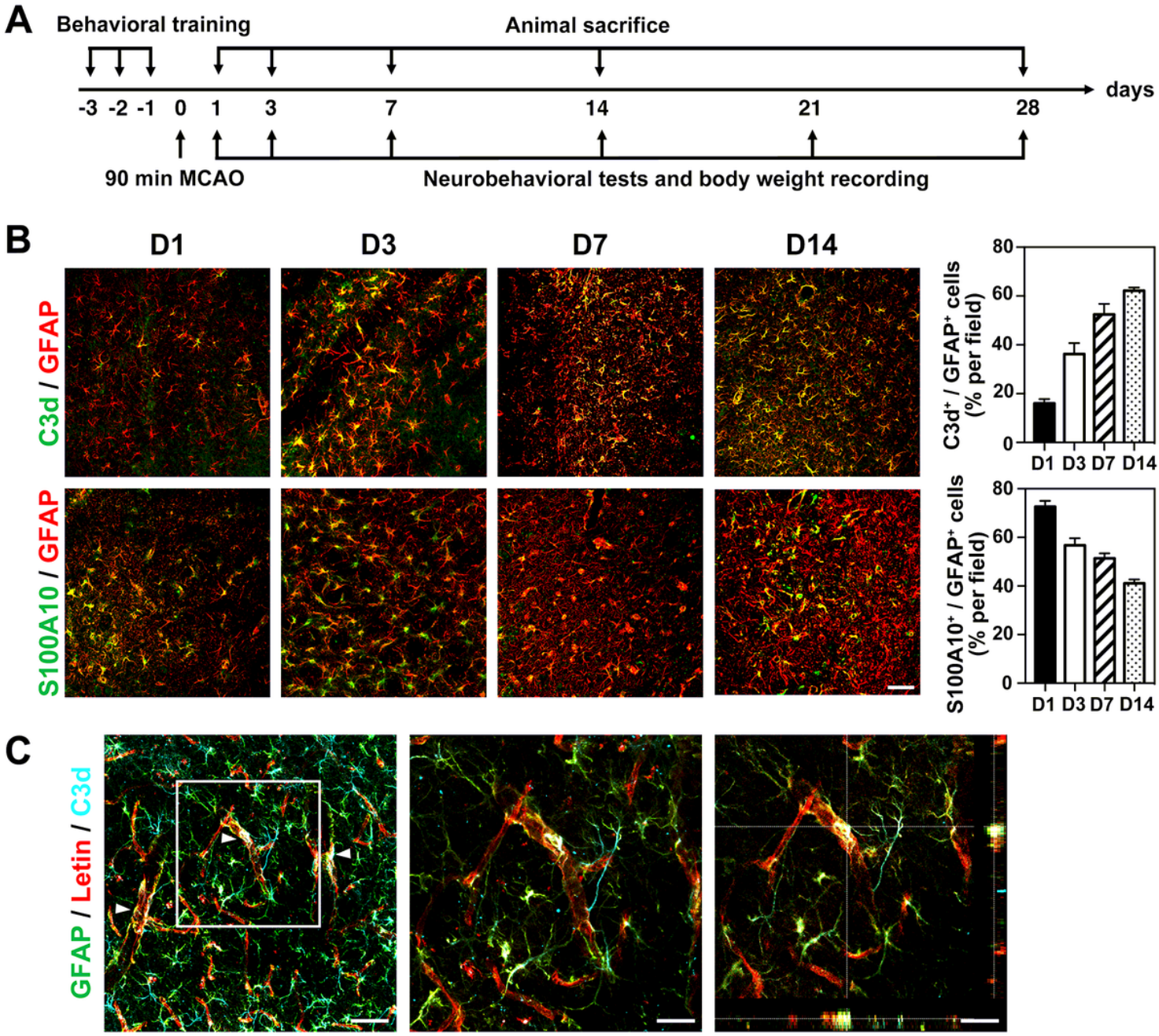

Figure 1

Phenotypic changes of astrocytes after tMCAO in mice a. Experimental scheme. Mice were trained for 3 days before tMCAO. Neurobehavioral tests and body weight were examined at 1, 3, 7, 14 and 28 days following tMCAO. Animals were sacrificed at 1, 3, 7, 14 and 28 days following tMCAO. b. Photomicrographs showed C3d+/GFAP+ cells (top, C3d in green color; GFPA in red color) and S100A10+/GFAP+ cells (bottom, S100A10 in green color; GFAP in red color) in the perifocal area of ipsilateral hemisphere at 1, 3, 7 and 14 days after tMCAO. Bar graph showed the percentage of C3d+/GFAP+ cells and S100A10+/GFAP+ in the ipsilateral hemisphere of brain at 1, 3, 7 and 14 days after tMCAO. Scale bar=50 μm. Data are mean±SEM, n=4-5 per group. c. Photomicrographs showed

C3d+/GFAP+ cells closely wrapped around lectin+ microvessels (arrowheads) in the perifocal area of the ipsilateral hemisphere in the mouse brain at 3 day after tMCAO. Scale bar=50 μm.

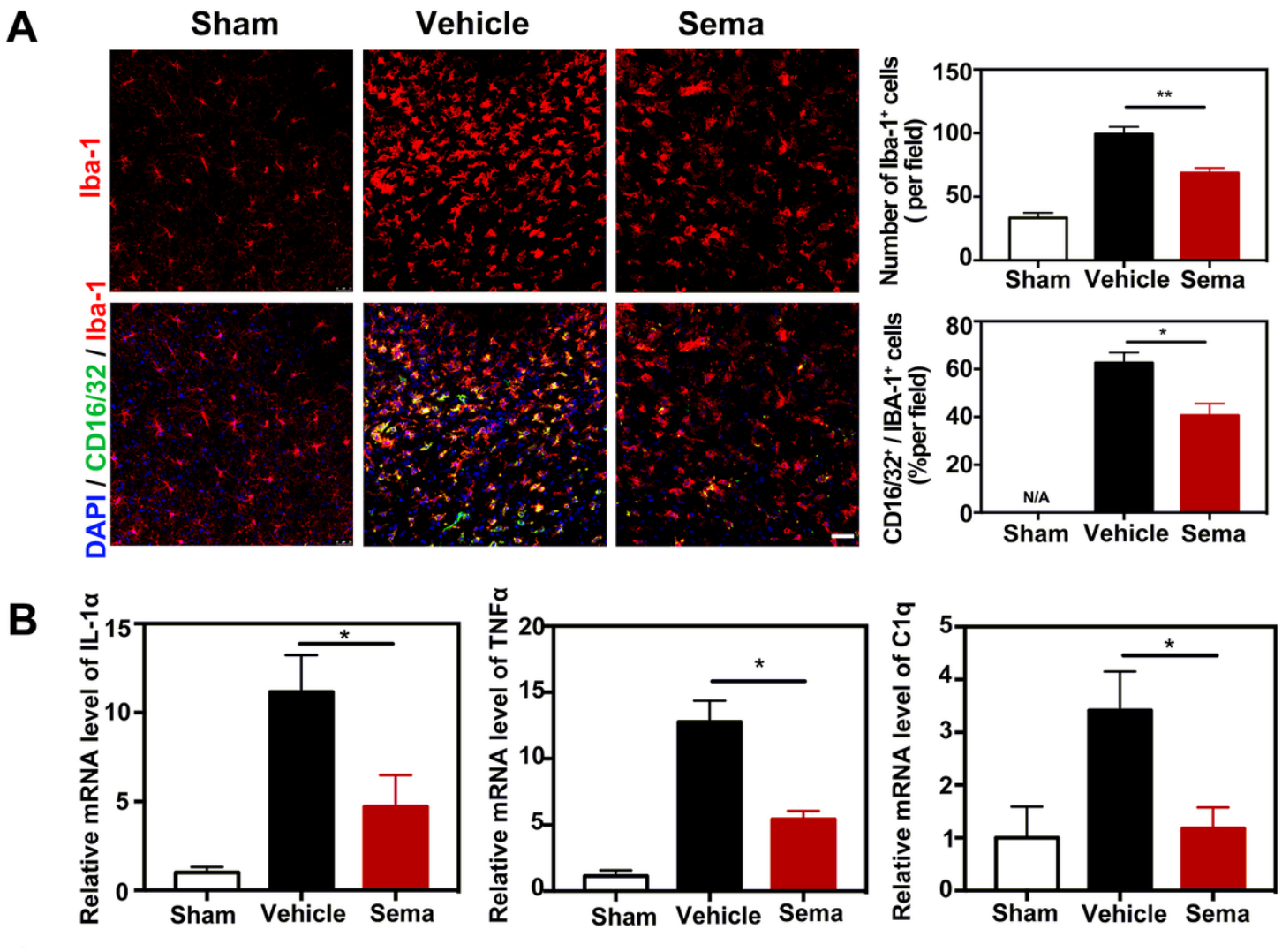

Figure 2

Semaglutide attenuated microglia M1 polarization after tMCAO a. Photomicrographs showed that CD16/32+/Iba-1+ cells (CD16/32 in green color; Iba-1 In red color) in the ipsilateral hemisphere of the perifocal area in sham mice, tMCAO mice and semaglutide treated tMCAO mice. Scale bar=25 μm. Bar graphs showed the number of Iba-1+ cells and CD16/32+/Iba-1+ cells in the perifocal area of ipsilateral hemisphere in the semaglutide treated tMCAO mice and control mice. Data are mean±SEM, n=3 per group. *p<0.05, **p<0.01. b. Bar graphs showed that the mRNA expression of IL-1α, TNFα and C1q in the perifocal area of ipsilateral hemisphere in the semaglutide treated tMCAO mice and the control mice at day 3 after tMCAO. Data are mean±SEM, n=4 per group, *p<0.05.

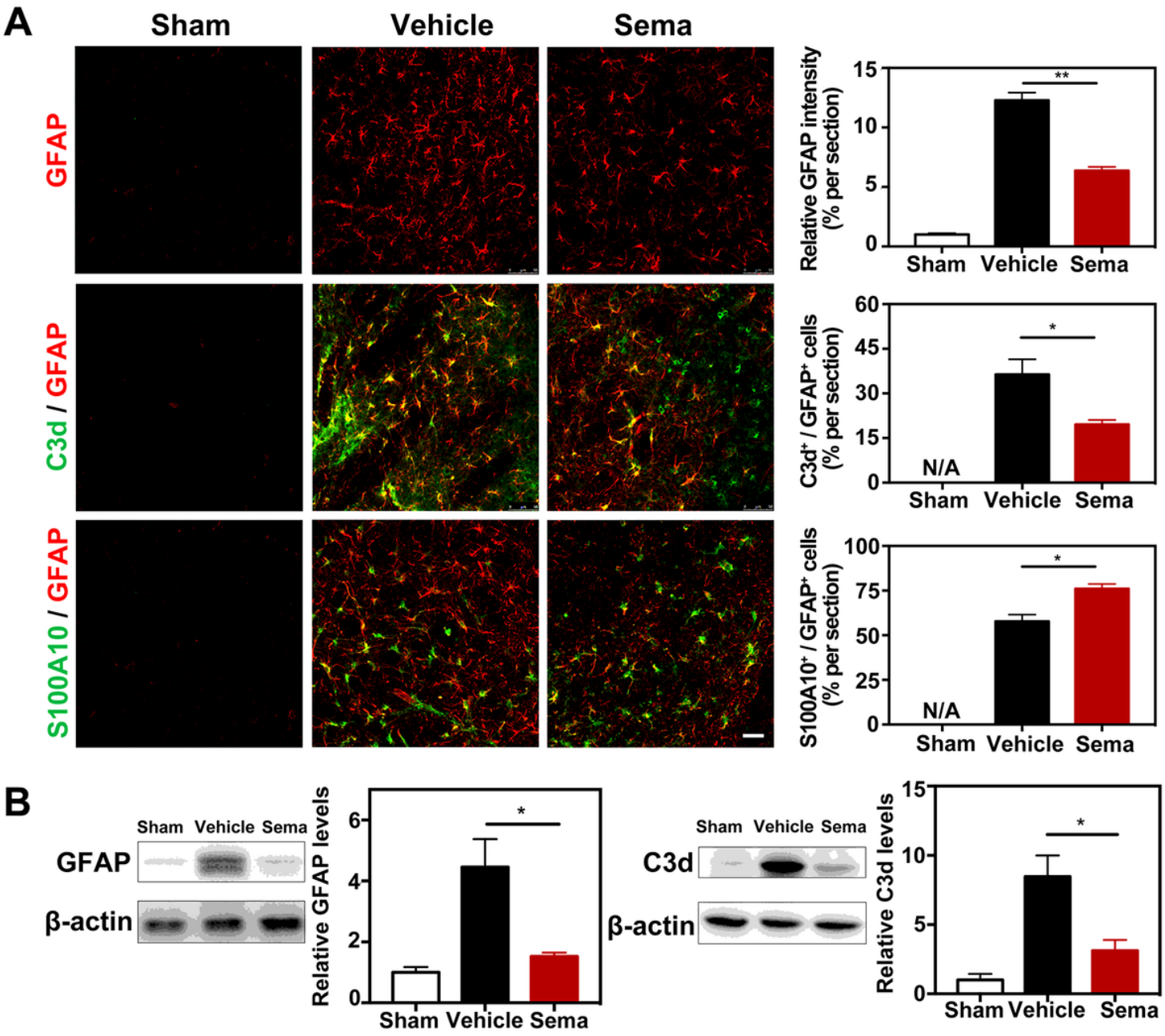

Figure 3

Semaglutide attenuated A1 reactive astrocyte transformation after tMCAO a. Representative photomicrographs showed that GFAP+ cells, C3d+/GFAP+ cells (C3d in green color; GFAP in red color) and S100A10+/GFAP+ cells (S100A10 in green color; GFAP in red color) in perifocal area of ipsilateral hemisphere in the semaglutide treated tMCAO mice and control mice at 3 days following tMCAO. Scale bar=50 μm. Bar graph showed that semi-quantification of GFAP intensity, the percentage of C3d+/GFAP+ cells, and S100A10+/GFAP+ cells. Data are presented as mean±SEM, n=3 per group. *p<0.05, **p<0.01. b. Western blotting analysis data showed relative GFAP and C3d levels in the perifocal area of ipsilateral hemisphere in the semaglutide treated tMCAO mice and control mice. Data are mean±SEM, n=3 per group. *p<0.05.

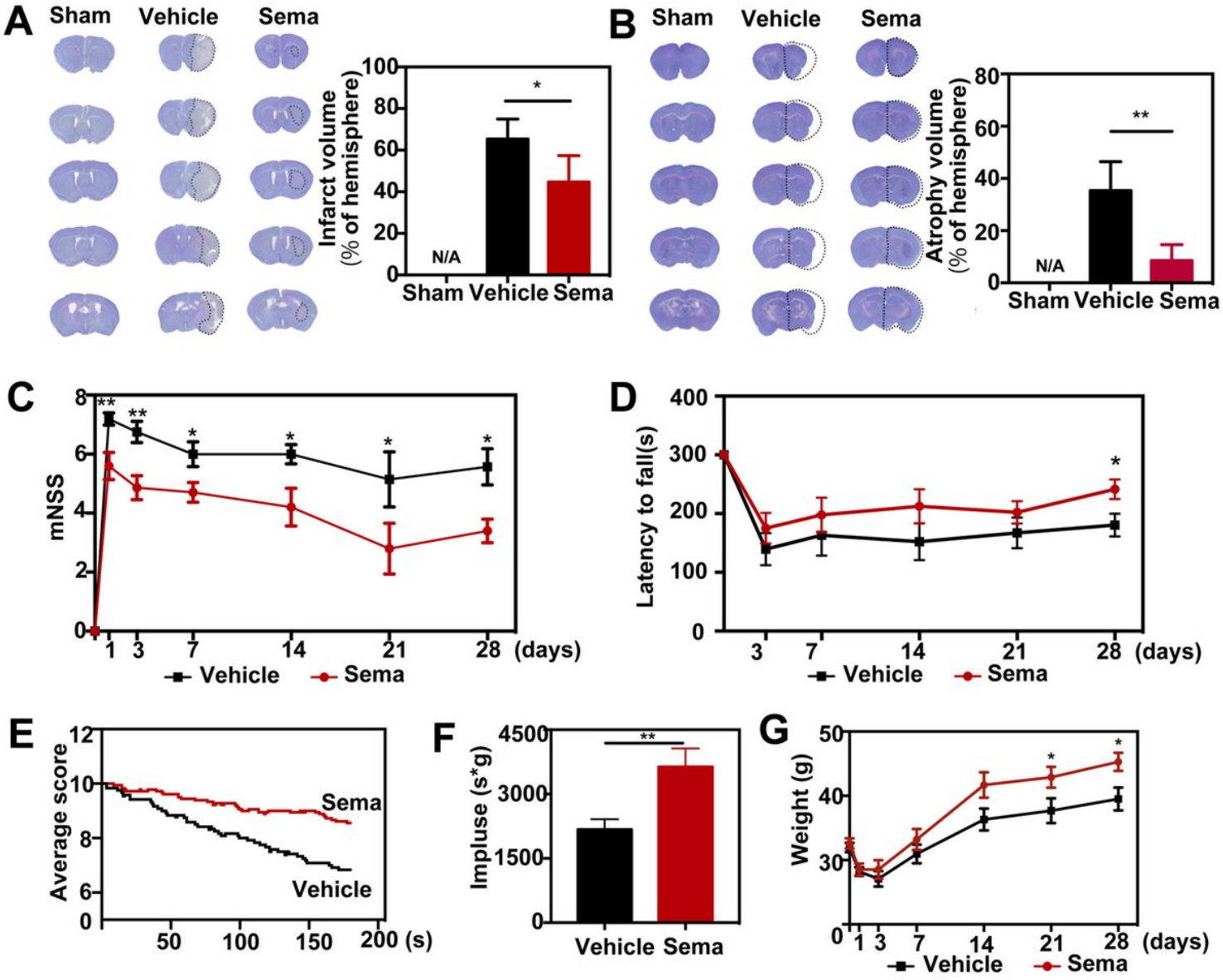

Figure 4

Inhibiting A1 astrocytes attenuated infarct volume and neurobehavioral deficit in the semaglutide treated tMCAO mice a-b. Cresyl violet-stained coronal sections of the brain in control mice, tMCAO mice, and semaglutide treated tMCAO mice following 3 (a, infarct) and 28 days (b, atrophy) of tMCAO. The brain infarct area and brain atrophy were circled by the dashed line. Bar graph showed the semi-quantitative analysis of the infarct volume and atrophy volume. Data are mean±SEM, n=6 per group. *p<0.05, **p<0.01. c-f. Neurobehavioral outcomes were assessed by three neurobehavioral tests including the modified neurological severity score (mNSS, c), rotarod test (d), and hanging wire test (e-f). Line graph showed body weight (g), Data are mean±SEM, n=9-12 per group, **p<0.01, *p<0.05.

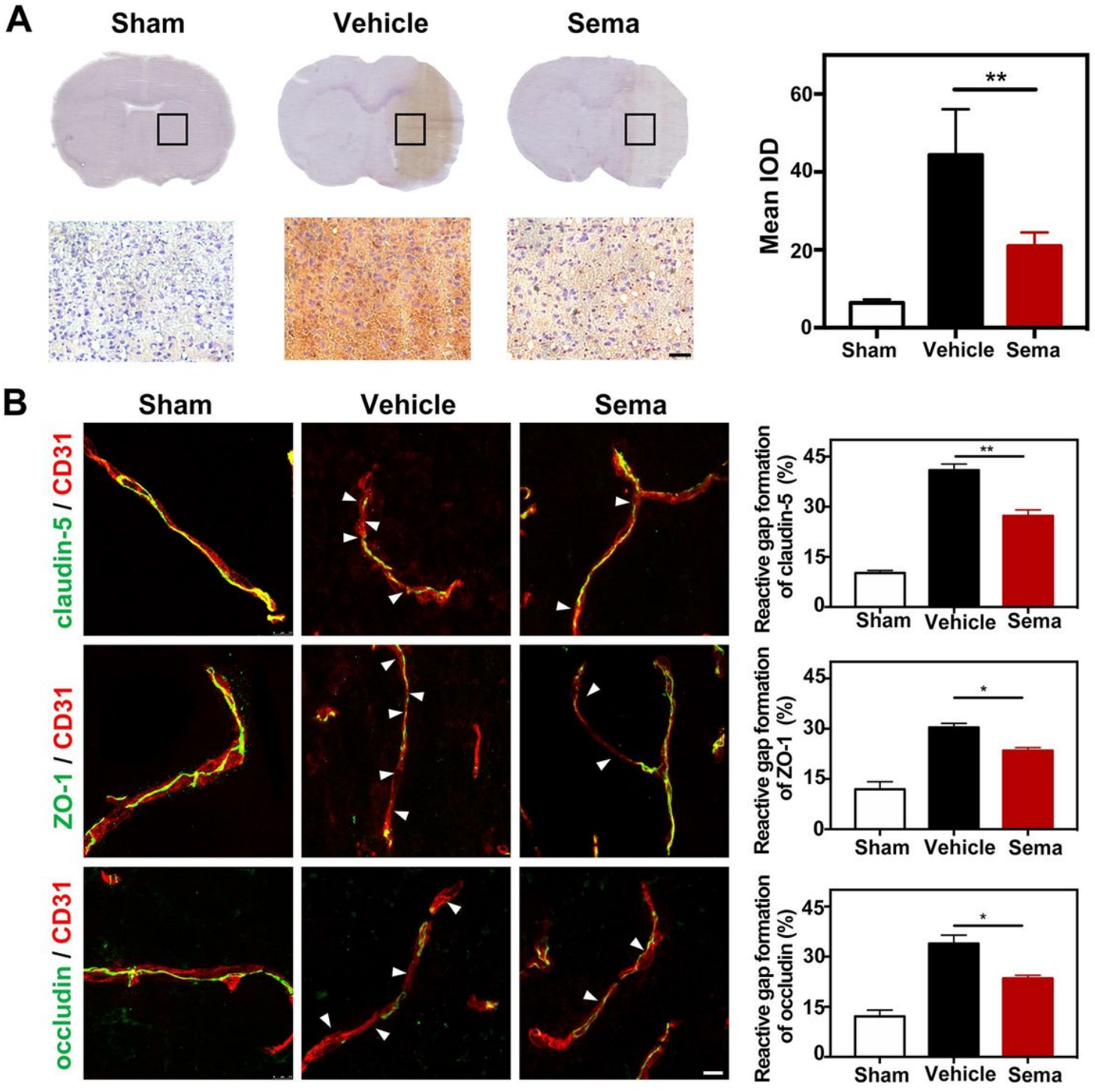

Figure 5

Inhibiting A1 astrocytes reduced BBB disruption and gap formation of tight junction in tMCAO mice a. Photographs showed IgG staining in the coronal section of the brain following 3 days of tMCAO in the semaglutide treated tMCAO mice, tMCAO mice, and control mice. Scale bar=50 μm. Bar graph showed the mean IOD of IgG intensity in these 3 groups. Data are mean±SEM, n=6 per group. **p<0.01. b. Photomicrographs showed CD31/claudin-5, CD31/ZO-1, and CD31/occludin double staining in the

ischemic peri-focal areas in the semaglutide treated tMCAO mice, tMCAO mice, and control mice. White arrows indicated discontinuous labeling and gap formation. Scale bar=10 μm. Bar graph showed relative gap formation of ZO-1, claudin-5, and occludin. Data are mean±SEM, n=3 per group. *p<0.05, **p<0.01.

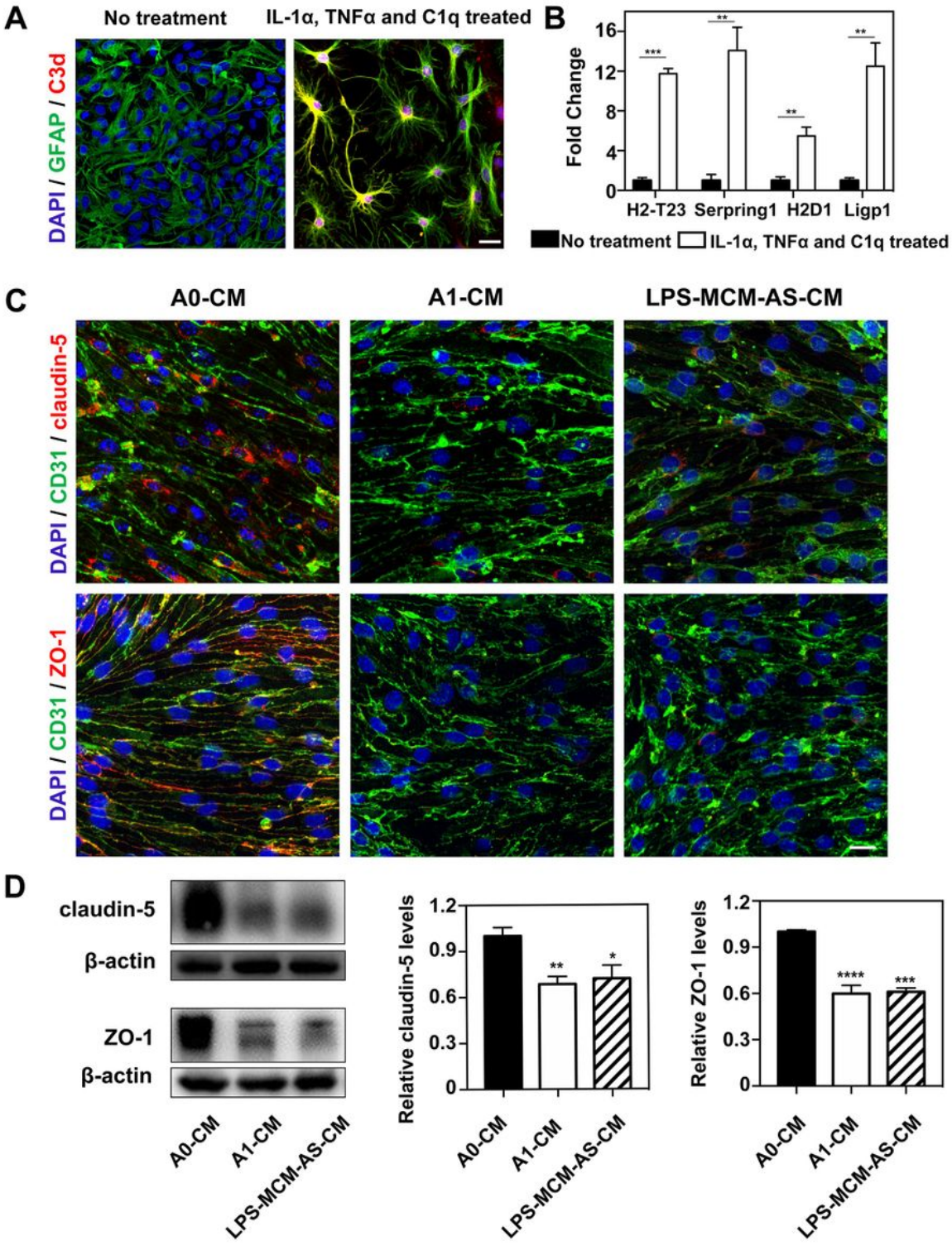

Figure 6

A1 astrocyte derived medium reduced tight junction protein expression in vitro a. Immunofluorescence images showed resting astrocytes were converted to C3d+/GFAP+ cells (C3d in red color; GFAP in green

color; DAPI in blue color) after treated with IL-1α, TNFα and C1q. Scale bar=25 μm. b. Bar graph showed the mRNA levels of C3d+/GFAP+ cells related genes H2-T23, Serping1, H2D1 and Ligp1 expression after IL-1α, TNFα and C1q treatment. Data are mean±SEM. n=3 per group. *p<0.05, ***p<0.001. c. Photomicrographs showed tight junction proteins (claudin-5 and ZO-1 in red color) expressed in CD31+ cells (green) that were treated by 1) medium derived from inactivated astrocytes (A0-CM), 2) medium derived from IL1α, TNFα and C1q treated astrocytes (A1-CM) and 3) medium derived from astrocytes that were treated with LPS-stimulated microglia (LPS-MCM-AS-CM). Scale bar=25 μm. d. Western blotting analysis of claudin-5 and ZO-1 in the A0-CM group, A1-CM group and LPS-MCM-AS-CM group. n=3 per group. *p<0.05, **p<0.01, ***p<0.001, ****p<0.0001.

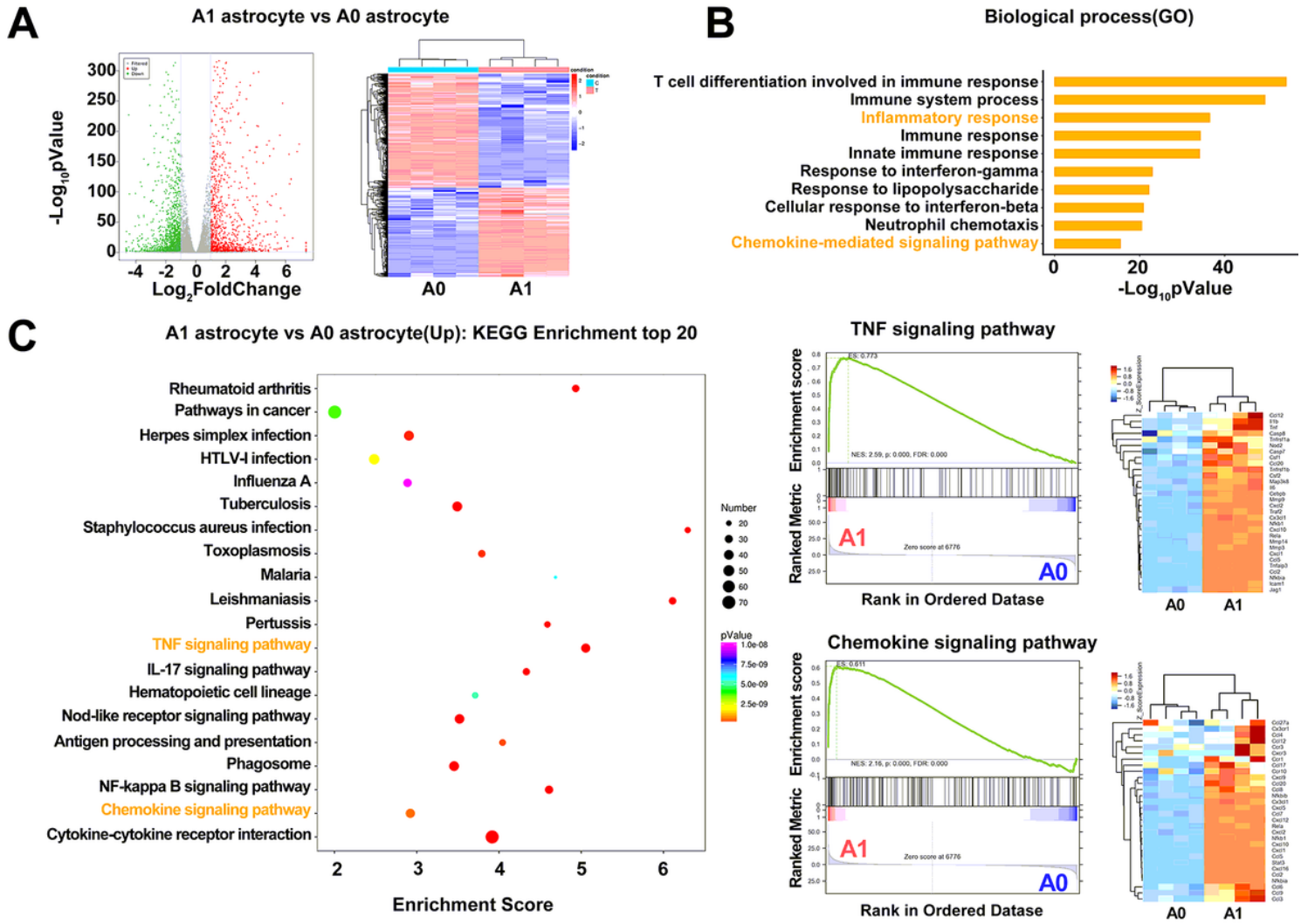

Figure 7

A1 astrocyte expressed different transcripts in RNA-seq data a. Volcano plot showed the upregulated (red) and downregulated (green) genes between A1 and A0 astrocyte. The horizontal axis is log2fold change, and the vertical axis is -log10p value, p<0.05. Heatmap showed the overall distribution of differentially expressed genes. Gene expression data was colored red for high expression and blue for low expression. b. GO enrichment analysis of differentially expressed genes based on RNA-seq data with p-

value showed top 10 upregulated biological process. c. KEGG enrichment top 20 analysis suggested that TNF signaling pathway and cytokine-cytokine receptor interaction were related with the phenotypic changes of astrocytes.

Supplementary Files

This is a list of supplementary files associated with this preprint. Click to download.

- Supplementarytable1.xlsx
- suppl.western.tif